

# Calculated optical properties of Si, Ge, and GaAs under hydrostatic pressure

M. Alouani and J. M. Wills

*Department of Physics, The Ohio State University, Ohio 43210-1368*

*Theoretical Division, Los Alamos National Laboratory Los Alamos, New Mexico 87545*

(June 16, 2018)

## Abstract

The macroscopic dielectric function in the random-phase-approximation without local field effect has been implemented using the local density approximation with an all electron, full-potential linear muffin-tin orbital basis-set. This method is used to investigate the optical properties of the semiconductors Si, Ge, and GaAs under hydrostatic pressure. The pressure dependence of the effective dielectric function is compared to the experimental data of Goñi and coworkers, and an excellent agreement is found when the so called “scissors-operator” shift (SOS) is used to account for the correct band gap at  $\Gamma$ . The effect of the  $3d$  semi-core states in the interband transitions hardly changes the static dielectric function,  $\epsilon_\infty$ ; however, their contribution to the intensity of absorption for higher photon energies is substantial. The spin-orbit coupling has a significant effect on  $\epsilon_\infty$  of Ge and GaAs, but not of Si. The  $E_1$  peak in the dynamical dielectric function is strongly underestimated for Si, but only slightly for Ge and GaAs, suggesting that excitonic effects might be important only for Si.

71.10.+x, 71.25.Tn, 78.20.-e

Typeset using REVTeX

## I. INTRODUCTION

The experimental determination of the optical properties of bulk semiconductors can now be obtained with high precision [1–3], yet our theoretical understanding is far from complete. The static dielectric constant, which can be obtained from a functional derivative of the electron density with respect to the total Kohn-Sham potential evaluated at the ground state, hence a ground state property, is over estimated by the local-density approximation (LDA) calculation [4–6]. The inclusion of the gradient correction to the pseudopotential LDA reduces slightly the discrepancy in the case of Silicon [7]. The underestimation of the  $E_1$  peak and the overestimation of the  $E_2$  peak of the imaginary part of the dielectric function,  $\epsilon_2(\omega)$ , by one-electron band theory have generated theoretical work for almost two decades to account for these discrepancies. It was clear from the beginning that including excitonic effects, which have been detected experimentally [8], could remove some of the disagreement with experiment [9–12]. However, the model calculations used to correct  $\epsilon_2(\omega)$  have produced only a qualitative understanding of the problem. In particular, the latest model by Hanke, Mattausch and Strinati based on the time-dependent screened Hartree-Fock approximation and including both the local field and the excitonic effects, described correctly the  $E_1$  peak but underestimated significantly the  $E_2$  peak of Si. The reason for the underestimation of  $E_2$  was attributed to a bad representation of the band structure of Si by their Slater-Koster parameterization [11]. Del Castello-Mussot and Sham [12] based their latest calculation on a  $\mathbf{k}\cdot\mathbf{p}$  model around the L point (where  $E_1$  originates) and a multiple plane-wave model around the X points (where  $E_2$  originates), and solved the Bethe-Salpeter equation containing the excitonic effect. Their model is an improvement over the non-interacting approximation: the  $E_1$  peak becomes stronger and the  $E_2$  peak weaker. This model is very promising, but, being based on a  $\mathbf{k}\cdot\mathbf{p}$  approximation to the band structure, it provided only a qualitative correction to the intensities of the  $E_1$  and  $E_2$  structures. Calculations ignoring excitonic effects, but including the local-field effect, underestimated both  $E_1$  and  $E_2$  peaks [13].

One way to make theoretical progress in this field is to determine the correct contribution

of the one-electron theory to the optical properties of semiconductors. This allows us to define precisely the size of the many body corrections to the one electron theory. However, a common belief these days is that the eigenvalues and vectors of the Kohn-Sham (KS) equations [14] have no direct physical meaning and hence should not be used to calculate optical spectra of materials. Only ground state properties derived from the total energy as a function of the electron density have in principle a direct physical meaning.

While LDA was indeed intended to calculate ground state properties it could also be viewed as a simplified quasi-particle (QP) theory where the self-energy is local and static ( $\Sigma(\mathbf{r}, \mathbf{r}', t) \approx V_{xc}(\mathbf{r})\delta(\mathbf{r} - \mathbf{r}')\delta(t)$ , here  $V_{xc}(\mathbf{r})$  is the local exchange and correlation potential as, for example, parameterized by Von Barth and Hedin [15]. The KS eigenvalues are then QP energies and could be compared to experimental data. This argument is supported by calculations using the GW approximation of Hedin [16]. These calculations showed that the valence QP energies of semiconductors are in good agreement with LDA and the conduction QP energies differ by approximately a rigid energy shift [17,18]. In the literature this shift is often called “scissors-operator” shift (SOS) [6].

First-principles local density approximation calculations started more than two decades ago, but the major problem of LDA, beside the well understood energy band gap problem [19], is the numerical difficulty to determine selfconsistent electronic structure and optical matrix elements using a complete basis-set. The early ab-initio calculation of the optical properties of semiconductors by Wang and Klein, using a selfconsistent linear combination of gaussian orbitals produced static dielectric functions in good agreement with experiment [20]. But this agreement is fortuitous because the band gaps produced by this method are much larger than the LDA band gaps. The recent calculations of 18 semiconductors by Huang and Ching using an orthogonalized linear combination of atomic orbitals method produced LDA static dielectric functions which are in general smaller than experiment despite the fact that their band gaps are much larger than the all-electron or pseudopotential LDA band gaps [21]. Those underestimated static dielectric constants are most likely due to the incompleteness of the basis-set used in their calculations.

Most of the theoretical studies of the optical properties of semiconductors in the literature use several approximations within the LDA, ranging from the use of spherical potentials [5] to the use of pseudopotentials [6] instead of all electron LDA potentials. In this paper we report precise calculations of the optical properties of bulk semiconductors Si, Ge, and GaAs under hydrostatic pressure using an all electron LDA linear muffin-tin orbital basis-set [22], in which no shape approximation is made for either the potential or the charge density [23]. The semi-core  $3d$  of Ga and Ge are included in a fully hybridizing valence basis set, and the rest of the core states are allowed to relax selfconsistently. The effect of spin-orbit coupling is also investigated. A systematic check of the  $f$ -sum rule is performed for all the calculations. We hope that this accurate LDA calculation will provide an excellent starting point for the determination of the local field and the excitonic effects in the optical spectra of semiconductors [9–13].

We have found that the static dielectric function,  $\epsilon_\infty$ , which is a ground state property, is overestimated by LDA over all pressure range, and that an excellent agreement with the experimental results of Goñi and coworkers [1] for  $\epsilon_\infty$  of GaAs and Ge under hydrostatic pressure is achieved only when the so-called scissors-operator shift is used to account for the correct band gap at  $\Gamma$ . The inclusion of the  $3d$  semi-core states of Ge and GaAs in the interband transition has almost no significant effects in  $\epsilon_\infty$ ; however, the  $3d$  interband transitions contribute significantly to the magnitude of  $\epsilon_2(\omega)$  above 25 eV for Ge, and above 12 eV for GaAs. The spin-orbit coupling increases the LDA values by about few percents.

The rest of the paper is organized as follows. In section II, we describe the method of calculation of electronic structure and the macroscopic dielectric function based on our all-electron full-potential LMTO basis-set. In section III we present the electronic properties of Si, Ge, and GaAs and compare them to existing theoretical results. The calculated dielectric functions and a discussion about including the semi-core states and the spin-orbit coupling will be presented in section IV. In the same section we also compare our static dielectric function under hydrostatic pressure with the experimental results of Goñi *et al.* [1]. The conclusion is given in Sec. V.

## II. METHOD OF CALCULATION

### A. All electron full-potential wave function

The full-potential linear muffin-tin orbital method in its scalar-relativistic and full-relativistic forms [23] is used here to calculate the electronic structure and the optical properties of Si, Ge, and GaAs under hydrostatic pressure. The Kohn-Sham [14] equations are solved for a general potential without any shape approximation [23]. In this subsection we describe the Bloch wave function inside the so-called muffin-tin spheres and the interstitial region. A correct determination of the crystal wave function is necessary for the accurate determination of the optical matrix elements.

As for the cellular methods, the space is divided into non-overlapping muffin-tin spheres surrounding atomic sites where the Schrödinger or the Dirac equation for each principle quantum number  $\nu$  and momentum channel  $\ell$  is solved for a fixed energy  $E_{\nu\ell}$ . In these muffin-tin spheres the trial wave function is linearized in terms of the solution of Schrödinger equation  $\phi_{\tau\ell}$  and its energy derivative  $\dot{\phi}_{\tau\ell}$  for the energy  $E_{\nu\ell}$ , and for an atom of type  $\tau$  and momentum channel  $\ell$  [22,24].

It can be shown that the Bloch wave function of site  $\tau$  calculated at site  $\tau'$  in the unit cell of the crystal at  $\mathbf{R} = \mathbf{0}$  is given by [23]:

$$\chi_{\tau\ell m}^{\mathbf{k}}(\mathbf{r})|_{\tau'} = \sum_{\ell'm'} \phi_{\tau'\ell'm'}(\mathbf{r} - \tau') B_{\ell'm',\ell m}^{(1)\tau\tau'}(\kappa, \mathbf{k}) + \dot{\phi}_{\tau'\ell'm'}(\mathbf{r} - \tau') B_{\ell'm',\ell m}^{(2)\tau\tau'}(\kappa, \mathbf{k}) \quad (1)$$

Where  $B_{\ell'm',\ell m}^{(1)\tau\tau'}(\kappa, \mathbf{k})$  and  $B_{\ell'm',\ell m}^{(2)\tau\tau'}(\kappa, \mathbf{k})$  are renormalized structure constants obtained from the crystal structure constants  $B_{\ell'm',\ell m}^{\tau\tau'}(\kappa, \mathbf{k})$  to ensure that the Bloch wave function is continuous and differentiable at the boundary of each muffin-tin sphere.

In the interstitial region, the muffin-tin orbitals are spherical wave solutions  $H_\ell$  to the Helmholtz equation with non-zero kinetic energy; these bases are Hankel functions for negative kinetic energies or Neumann functions for positive kinetic energies  $\kappa^2$ . Such that each partial wave inside the muffin-tin sphere is allowed to have different kinetic energy,  $\kappa^2$ , in the interstitial region. In this region the Bloch wave function is given by:

$$\chi_{\tau\ell m}^{\mathbf{k}}(\mathbf{r}) = \sum_{\mathbf{R}} e^{i\mathbf{k}\mathbf{R}} H_{\ell}(\kappa, |\mathbf{r} - \tau - \mathbf{R}|) i^{\ell} Y_{\ell m}(\widehat{\mathbf{r} - \tau - \mathbf{R}}) \quad (2)$$

The interstitial-region Bloch function is expressed in plane waves over the reciprocal lattice using Fourier transform :

$$\chi_{\tau\ell m}^{\mathbf{k}}(\mathbf{r}) = \sum_{\mathbf{G}} f_{\mathbf{K}}(\mathbf{k} + \mathbf{G}) e^{i(\mathbf{k} + \mathbf{G})\mathbf{r}} \quad (3)$$

Where  $\mathbf{K} = \{\tau, \ell, m, E_{\ell}, \kappa\}$ , here the parameter  $E_{\ell}$  is the linearization energy of the wave function in the muffin-tin sphere for the  $\ell$  momentum channel,  $m$  is the azimuthal quantum number, and  $\kappa$  is the variational parameter whose square is the kinetic energy in the interstitial region. The Fourier coefficients,  $f_{\mathbf{K}}$ , are obtained from a pseudo-wave function that is equal to the crystal wave function in the interstitial region and represented by a smooth function inside the muffin-tin spheres. The exact shape of these pseudo-functions inside the muffin-tin spheres is not important. The only requirement is that they are continuous and differentiable at the sphere boundary and have zero slope at the origin of each sphere. The plane wave expansion is multiplied by a three dimensional step function so that the wave function is kept only in the interstitial region. The knowledge of the Bloch wave function in the whole unit cell allows us to calculate the Hamiltonian and overlap matrix elements in order to solve the effective one electron Schrödinger equation.

Three different kinetic energies were used for each subset of  $s$  and  $p$  derived bases in the basis set; two kinetic energies were used for bases derived from orbital parameters  $\ell \geq 1$ . The basis sets used in calculating total energies and structural properties were for Si: 3(3s3p), 2(3d), for Ge: 2(3d), 3(4s4p), 2(4d), and for GaAs: 2(Ga 3d), 3(Ga 4s4p), 2(Ga 4d), 3(As 4s4p), 2(As 4d); the pre-multiplicities in this notation refer to the number kinetic energies used in this basis subset. The basis functions for each material comprised a single, fully hybridizing basis set. Note the presence of both 3d and 4d derived bases on Ga and Ge. A useful feature of the method used in these calculations is the ability to incorporate basis functions derived from the same orbital atomic quantum numbers but different principal atomic quantum numbers in a single fully hybridizing basis set. This feature entails the use of multiple sets of radial functions to represent bases with different principle atomic quantum

numbers. This capability was particularly useful in calculating the high-lying energy bands which were used to obtain the dielectric functions to high energy; the basis sets employed for this purpose are given in Table I. Seven to eight kinetic energies were used in the basis sets. Accurate resolution of the bands to high energy was necessary to converge the calculation of the real part of the dielectric function, which was obtained from the imaginary part through the Kramers-Kronig relation. An interesting consequence of the relaxation of the Ga  $3d$  states as valence states is a significant decrease in the calculated band gap [25].

For the core charge density, the Dirac equation is solved selfconsistently, e.g., no frozen core approximation is used. The exchange and correlation potential is treated within the Von Barth and Hedin parameterization [15]. To account for the relativistic effects in the dielectric function, the full-selfconsistent relativistic band structure is produced by including the spin-orbit coupling to the Hamiltonian. In Table I we show the orbitals used to describe the electronic states of Si, Ge, and GaAs. This large number of orbitals is necessary to calculate accurately the eigenvalues and eigenvectors up to 5 Ry above the highest valence states. These electronic states will be needed to determine the dynamical dielectric function and the converged static dielectric function through the use of Kramers-Kronig relations.

The completeness of basis-set, with different variational  $\kappa$  values for each partial wave in the interstitial region together with the Fourier representation allows the method to treat open structures like the zinc-blende structure studied here without having to resort to the so-called empty spheres [26]. The high energy states are also determined more accurately due to the use of many  $\kappa$  values. As a test we show in Table II the eigenvalues of Si at high symmetry points of the Brillouin zone compared with some recent results from first principle calculations based on ab-initio pseudopotential and Gaussian orbital methods [27,28]. The agreement of our calculation with the previous calculations is excellent.

## B. Dielectric Function

Here we give a concise review of the determination of the dielectric function of a semiconductor crystal due to the application of an electric field. We also determine the approximations used to obtain numerical results for Si, Ge, and GaAs under hydrostatic pressure with or without scissors-operator shift.

A perturbative electromagnetic field of frequency  $\omega$ , and a wave vector  $\mathbf{q} + \mathbf{G}$  on a crystal produces a response of frequency  $\omega$  and a wave vector  $\mathbf{q} + \mathbf{G}'$  ( $\mathbf{G}$  and  $\mathbf{G}'$  being reciprocal lattice vectors). The microscopic field of wave vector  $\mathbf{q} + \mathbf{G}'$  is produced by the umklapp processes as a result of the applied field  $E_0(\mathbf{q} + \mathbf{G}, \omega)$

$$E_0(\mathbf{q} + \mathbf{G}, \omega) = \sum_{\mathbf{G}'} \epsilon_{\mathbf{G}, \mathbf{G}'}(\mathbf{q}, \omega) E(\mathbf{q} + \mathbf{G}', \omega) \quad (4)$$

where  $E(\mathbf{q} + \mathbf{G}, \omega)$  is the total field which produces the non-diagonal elements in the microscopic dielectric function  $\epsilon_{\mathbf{G}, \mathbf{G}'}(\mathbf{q}, \omega)$ . In the random phase approximation the microscopic dielectric function is given by [29]:

$$\begin{aligned} \epsilon_{\mathbf{G}, \mathbf{G}'}(\mathbf{q}, \omega) = & \delta_{\mathbf{G}, \mathbf{G}'} - \frac{8\pi e^2}{\Omega |\mathbf{q} + \mathbf{G}| |\mathbf{q} + \mathbf{G}'|} \sum_{\mathbf{k}, n, n'} \frac{f_{n', \mathbf{k} + \mathbf{q}} - f_{n, \mathbf{k}}}{E_{n', \mathbf{k} + \mathbf{q}} - E_{n, \mathbf{k}} - \hbar\omega + i\delta} \langle n', \mathbf{k} + \mathbf{q} | e^{i(\mathbf{q} + \mathbf{G})\mathbf{r}} | n, \mathbf{k} \rangle \\ & \times \langle n, \mathbf{k} | e^{-i(\mathbf{q} + \mathbf{G}')\mathbf{r}} | n', \mathbf{k} + \mathbf{q} \rangle \end{aligned} \quad (5)$$

Here  $n$  and  $n'$  are the band indexes,  $f_{n, \mathbf{k}}$  is the zero temperature Fermi distribution, and  $\Omega$  is the cell volume. The energies  $E_{n, \mathbf{k}}$  and the the crystal wave function  $|n, \mathbf{k}\rangle$  are produced for each band index  $n$  and for each wave vector  $\mathbf{k}$  in the Brillouin zone.

The macroscopic dielectric function in the infinite wave length limit is given by the inversion of the microscopic dielectric function:

$$\begin{aligned} \epsilon(\omega) = & \lim_{\mathbf{q} \rightarrow \mathbf{0}} \frac{1}{[\epsilon_{\mathbf{G}, \mathbf{G}'}^{-1}(\mathbf{q}, \omega)]_{\mathbf{0}, \mathbf{0}}} \\ = & \epsilon_{\mathbf{0}, \mathbf{0}}(\omega) - \lim_{\mathbf{q} \rightarrow \mathbf{0}} \sum_{\mathbf{G}, \mathbf{G}' \neq \mathbf{0}} \epsilon_{\mathbf{0}, \mathbf{G}}(\mathbf{q}, \omega) T_{\mathbf{G}, \mathbf{G}'}^{-1}(\mathbf{q}, \omega) \epsilon_{\mathbf{G}', \mathbf{0}}(\mathbf{q}, \omega) \end{aligned} \quad (6)$$

Where  $T_{\mathbf{G}, \mathbf{G}'}^{-1}$  is the inverse matrix of  $T_{\mathbf{G}, \mathbf{G}'}$  containing the elements  $\epsilon_{\mathbf{G}, \mathbf{G}'}$  with  $\mathbf{G}$  and  $\mathbf{G}' \neq \mathbf{0}$ . The first term of this equation is the interband contribution to the macroscopic



dielectric function and the second term represent the local-field correction to  $\epsilon$ . The most recent ab-initio pseudopotentials calculation found that the local-field effect reduces the static dielectric function by at most 5% [6]. Previous calculations with the same method have also found a decrease of  $\epsilon_\infty$  by about the same percentage [4,17]. We are looking at the effect of the local field using our all-electron basis-set; it should be of interest to compare all electron results with these obtained using the pseudopotential method.

For insulators the dipole approximation of the imaginary part of the first term of equation (7) is given by [30]:

$$\epsilon_2(\omega) = \frac{e^2}{3\omega^2\pi} \sum_{n,n'} \int d\mathbf{k} |\langle n, \mathbf{k} | \mathbf{v} | n', \mathbf{k} \rangle|^2 f_{n,\mathbf{k}} (1 - f_{n',\mathbf{k}}) \delta(e_{\mathbf{k},n',n} - \hbar\omega), \quad (7)$$

Here  $\mathbf{v}$  is the velocity operator, and in the LDA  $\mathbf{v} = \mathbf{p}/m$  ( $\mathbf{p}$  being the momentum operator), and where  $e_{\mathbf{k},n,n'} = E_{n',\mathbf{k}} - E_{n,\mathbf{k}}$ . The matrix elements  $\langle n\mathbf{k} | \mathbf{p} | n'\mathbf{k} \rangle$  are calculated for each projection  $p_j = \frac{\hbar}{i} \partial_j$ ,  $j = x$  or  $y$  and  $z$ , with the wave function  $|n\mathbf{k}\rangle$  expressed in terms of the full-potential LMTO crystal wave function described by equations (1) and (3). The  $\mathbf{k}$ -space integration is performed using the tetrahedron method [31] with 480 irreducible  $\mathbf{k}$  points the whole Brillouin zone. The irreducible  $\mathbf{k}$ -points are obtained from a shifted  $\mathbf{k}$ -space grid from the high symmetry planes and  $\Gamma$  point by a half step in each of the  $k_x$ ,  $k_y$ , and  $k_z$  directions. This scheme produces highly accurate integration in the Brillouin zone by avoiding high symmetry points.

To calculate these matrix elements we first defined a tensor operator of order one out of the momentum operator  $\nabla_0 = \nabla_z = \frac{\partial}{\partial z}$  and  $\nabla_{\pm 1} = \mp \frac{1}{\sqrt{2}} (\frac{\partial}{\partial x} \pm i \frac{\partial}{\partial y})$ . The muffin-tin part of the momentum matrix elements is calculated using the commutator  $[\nabla^2, x_\mu] = 2\nabla_\mu$  so that:

$$\int_{S_\tau} d\mathbf{r} \phi_{\tau\ell'}(r) Y_{\ell'm'}(\widehat{\mathbf{r}} - \tau) \nabla_\mu \phi_{\tau\ell}(r) Y_{\ell m}(\widehat{\mathbf{r}} - \tau) = -\frac{i}{2} G_{\ell m, \ell', m'}^{1\mu} \int_0^{S_\tau} r^2 dr \phi_{\tau\ell'} \left( \frac{2}{r} \frac{d}{dr} r + \frac{\ell(\ell+1) - \ell'(\ell'+1)}{r} \right) \phi_{\tau\ell}(r) \quad (8)$$

where  $G_{\ell m, \ell', m'}^{1\mu}$  are the usual Gaunt coefficients, and  $S_\tau$  is the radius of the muffin-tin sphere of atom  $\tau$ . In the interstitial region the plane-wave representation of the wave function (see

equation 3) makes the calculation straightforward, but a special care has to be taken for the removal of the extra contribution in the muffin-tin spheres. However, we find it much easier and faster to transform the interstitial matrix elements as an integral over the surface of the muffin-tin spheres using the commutation relation of the momentum operator and the Hamiltonian in the interstitial region. The calculation of the interstitial momentum matrix elements is then similar to the calculation of the interstitial overlap matrix elements [23]. The  $\kappa = 0$  case has been already derived by Chen using the Korringa, Kohn and Rostoker Green's-function method [32]. We have tested that both the plane-wave summation and the surface integration provide the same results.

Equation (7) can not be used directly to determine the optical properties of semiconductors, when the GW approximation or the scissors operator is used to determine the electronic structure. The velocity operator should be obtained from the effective momentum operator  $\mathbf{p}^{\text{eff}}$  which is calculated using the self-energy operator,  $\Sigma(\mathbf{r}, \mathbf{p})$ , of the system [33]:

$$\mathbf{v} = \mathbf{p}^{\text{eff}}/m = \mathbf{p}/m + \partial\Sigma(\mathbf{r}, \mathbf{p})/\partial\mathbf{p} \quad (9)$$

GW calculations show that the quasiparticle wave function is almost equals to the LDA wave function [17,18]. Based on this assumption, Del Sole and Girlanda show that the effective momentum operator  $\mathbf{p}^{\text{eff}}$  can be written in terms of the momentum operator  $\mathbf{p}$  as follows [33]:

$$\langle n', \mathbf{k} | \mathbf{p}^{\text{eff}} | n, \mathbf{k} \rangle = \langle n', \mathbf{k} | \mathbf{p} | n, \mathbf{k} \rangle e_{\mathbf{k}, n', n}^{QP} / e_{\mathbf{k}, n', n}, \quad (10)$$

where  $e_{\mathbf{k}, n', n}^{QP} = E_{n', \mathbf{k}}^{QP} - E_{n, \mathbf{k}}^{QP}$  is the difference between the quasiparticle energy  $E_{n', \mathbf{k}}^{QP}$  of the unoccupied state  $|n', \mathbf{k}\rangle$  and the occupied state  $|n, \mathbf{k}\rangle$ . By substituting Equation 10 into equation 7, it can be easily shown [33] that in the case of the scissors operator, where all the empty states are shifted rigidly by a constant energy  $\Delta$ , the imaginary part of the dielectric function is a simple energy shift of the LDA dielectric function towards the high energies by an amount  $\Delta$ , i.e.,  $\epsilon_2^{QP}(\omega) = \epsilon_2^{\text{LDA}}(\omega - \Delta/\hbar)$ . The real part of the dielectric function is then obtained from the shifted  $\epsilon_2$  using Kramers-Kronig relations. The expression of  $\epsilon_\infty^{QP}$  is given by:

$$\epsilon_{\infty}^{QP} = 1 + \frac{2e^2}{3\omega^2\pi^2} \sum_{n,n'} \int d\mathbf{k} f_{n,\mathbf{k}}(1 - f_{n',\mathbf{k}}) \frac{|\langle n, \mathbf{k} | \mathbf{p} | n', \mathbf{k} \rangle|^2}{(e_{\mathbf{k},n',n} + \Delta)e_{\mathbf{k},n',n}^2}, \quad (11)$$

$\epsilon_{\infty}^{QP}$  is very similar to  $\epsilon_{\infty}^{LDA}$  except that one of the interband gap  $e_{\mathbf{k},n',n}$  is substituted by the QP interband gap  $e_{\mathbf{k},n',n} + \Delta$ .

To test for the accuracy of the calculation within the LDA the f-sum rule:

$$\frac{2}{3mn_v} \sum_{\mathbf{k}} \sum_{n,n'} f_{n,\mathbf{k}}(1 - f_{n',\mathbf{k}}) \frac{|\langle n, \mathbf{k} | \mathbf{p} | n', \mathbf{k} \rangle|^2}{e_{\mathbf{k},n',n}} = 1, \quad (12)$$

where  $n_v$  is the number of valence bands, is checked in all the calculations, and it is satisfied to within a few percent.

It is easily seen that the dielectric function  $\epsilon_2^{QP}$  calculated using the scissors-operator shift does not satisfy the sum rule ( $\omega_P$  is the free-electron plasmon frequency):

$$\int_0^{\infty} \omega \epsilon_2(\omega) d\omega = \frac{\pi}{2} \omega_P^2 \quad (13)$$

because (i)  $\epsilon_2^{LDA}$  satisfies this rule, and (ii)  $\epsilon_2^{QP}$  is obtained by a simple shift of  $\epsilon_2^{LDA}$  by the scissors-operator  $\Delta$  towards higher energies. Using the expression of the quasiparticle dielectric function in the scissors-operator shift approximation we show that  $\epsilon_2^{QP}$  satisfy the following integral sum rule:

$$\int_0^{\infty} \omega \epsilon_2^{QP}(\omega) d\omega = \frac{\pi}{2} \omega_P'^2 \quad (14)$$

where  $\omega_P'^2 = \omega_P^2 + \frac{2e^2\Delta}{3\pi^2m^2} \sum_{n,n'} \int d\mathbf{k} |\langle n, \mathbf{k} | \mathbf{p} | n', \mathbf{k} \rangle|^2 / e_{\mathbf{k},n',n}^2 f_{n,\mathbf{k}}(1 - f_{n',\mathbf{k}})$ . We recover the usual sum rule when  $\Delta$  is equal to zero. The non simultaneous satisfaction of both the f-sum rule and the integral sum rule given by Eq. 13 within the scissors approximation shows the limitation of this approximation. While the scissors operator approximation describes nicely the low lying excited states, which is seen in the good determination of the static dielectric function and the low energy structures, i.e.  $E_1$  and  $E_2$ , in the imaginary part of the dielectric function, it seems to fail for the description of the higher excited states. This is not surprising because the higher excited states which are free electrons like are most probably well described by LDA and need no scissors operator shift. This is supported by the

fact that the the energy-loss function,  $-\text{Im}\epsilon^{-1}$ , within the LDA has its maximum roughly at the free electron plasmon frequency whereas within the scissors approximation its maximum is shifted to higher energies as given by equation (14). Fig. 1 shows the energy-loss function of GaAs calculated within LDA (full curve) and within the scissors approximation (dashed curve). It is clearly seen that the maximum of the LDA curve has a maximum which is closer to the free valence electron plasma frequency of 15.5 eV. It is of general interest to see whether the calculated dielectric function within the GW approximation satisfies the integral sum rule. For our purpose the scissors-operator shift remains a good approximation for the description of the low-lying excited states of semiconductors and their optical properties.

### III. ELECTRONIC STRUCTURE OF SI, GE, AND GAAS

The electronic structure of Si, Ge, and GaAs are obtained by solving the LDA equations by means of a full-potential LMTO basis-set as described above. Table I shows the orbitals used to describe the valence and conduction bands during the selfconsistency. The large number of orbitals used is found necessary to obtain converged excited states up to 5 Ry above the top of the valence states. However the total energy is insensitive to these high energy orbitals, but the presence of the  $3d$ -core states of Ge and GaAs are important [25].

Table II compares our band structure of Si for some high symmetry points with some recent results from first-principles calculations based on pseudopotential and Gaussian orbitals methods [27,28]. We found a good agreement between our results and these calculations. This reflects the high accuracy of our unoccupied states which are used to determine the dynamical dielectric function.

Table III shows the calculated equilibrium structural parameters, i.e., the electronic pressure and the bulk modulus at the experimental unit cell volume,  $V_0$ , and calculated cell volume,  $V$ . The calculated equilibrium volume  $V$  is at the most 2% smaller than the experimental value which correspond to a less than 0.5% deviation from the experimental lattice parameter. However the bulk modulus which is very sensitive to the slope of the

total energy versus the unit cell volume deviates at the most by 10% in the case of Ge, and when calculated at the experimental unit cell volume. But only by 5% when calculated at the theoretical equilibrium volume. Our calculation of the bulk modulus is in excellent agreement with other calculation [34].

Figure 2 shows the LDA underestimated (a) direct band and (b) minimal gaps of Si, Ge, and GaAs compared with the Ge, and GaAs experimental results of Goñi et al. [1]. For GaAs a cross over from direct band gap to indirect band gap takes place between  $\Gamma$  and  $X$  at approximately 8 GPa. For Ge this cross over occurs along  $\Gamma L$  at a lower pressure of 3 GPa. The direct band gap increases linearly with pressure and is in good agreement with the experimental results for both GaAs and Ge. There is no experimental data for Si under hydrostatic pressure. Table IV present the first and second order coefficients describing the dependence of the direct band gap at  $\Gamma$  under hydrostatic pressure,  $E_0(P) = E_0 + aP + bP^2$ , compared to the experimental results of Goñi et al. [1]. Apart for the underestimation of the band gap, the first and second coefficients of the pressure dependence of the band gap are in good agreement with the experimental results. This suggest that the scissors-operator shift is a good approximation for the description of the band gap under hydrostatic pressure.

#### IV. OPTICAL PROPERTIES OF SI, GE, AND GAAS

##### A. frequency dependent of the complex dielectric function of Si, Ge, and GaAs

Figure 3 and 4 present the imaginary part of the macroscopic dielectric function of Si, Ge, and GaAs obtained at the experimental ground state lattice parameters except for Ge where we have compressed the lattice parameter by about 1%. The compression is done because within LDA and at the experimental lattice parameter Ge is a semi-metal. The LDA  $\epsilon_2$  is shifted towards higher energy by the scissors-operator shift in order that the optical band gap agrees with experiment. The comparison to experimental results of Aspnes and Studna [3] shows that all the features in the experimental spectra are reproduced by

the calculation. It is interesting to notice that the calculated LDA  $\epsilon_2(\omega)$  of Si exhibit the largest underestimation of the  $E_1$  peak (about 50% in intensity) whereas, in Ge and GaAs the underestimation of the  $E_1$  peak is only about 12%. The  $E_2$  peak is overestimated by LDA by about 34% for Si, 50% for Ge, and 60% for GaAs. This overestimation of the  $E_2$  peak by LDA is due to a strong van Hove singularity near the X points of the Brillouin zone where parallel bands occur over a large plateau [5,35]. This overestimation can be reduced substantially by including the life-time broadening of the quasiparticles through a self-energy calculation.

The effect of interband electronic transitions due to the  $3d$  semi-core states, without scissors operator shift, is presented in Fig. 5a and refeps2highb for Ge, and GaAs respectively. For Ge the onset of transitions begun at photon energy of about 25 eV, and the intensity is very similar to the  $p$ -density of states of the empty states of Ge. This is because the  $3d$  states of Ge are very narrow, and the dipole selection rules allow transitions only to the empty  $p$  states of Ge, the  $f$ -states in this energy range are absent. Whereas for GaAs, the onset of transitions begun at 12 eV, and the intensity  $\epsilon_2$  spectrum above 12 eV is very different from the empty  $p$  states of Ga. This is because of the relatively large dispersion of the  $3d$  semi-core states of Ga. It should be of interest to confirm experimentally these theoretical predictions.

The real part  $\epsilon_1(\omega)$  of the dielectric function of Si, Ge, and GaAs calculated by Kramers-Kronig transform of the imaginary part  $\epsilon_2(\omega)$  are presented in Fig. 6 together with the experimental results of Aspnes and Studna [3]. In the same figure we have also presented the scissors-operator shift  $\epsilon_1^{QP}(\omega)$  and the high frequency asymptotic limit  $\epsilon_1(\omega) = 1 - \omega_P^2/\omega^2$ , where  $\omega_P$  is the free-electron plasmon frequency. We notice that the analytic asymptotic limit matches nicely the calculated LDA  $\epsilon_1$ , which is an indication of the quality of the calculation. For the  $\epsilon_1^{QP}$  we need to use a different plasmon frequency as described in equation (14) due to the poor description of the higher excited states by the scissors approximation.

In conclusion, we believe that the excitonic effects may be important for the dielectric function of Si but less for those of Ge, and GaAs. A QP calculation of the dielectric function

including the dynamical screening of the Coulomb interaction, like in the GW approximation of Hedin [16], would certainly improve the intensity of at least the  $E_2$  peak by introducing a life-time broadening of the quasi-particles.

## **B. Hydrostatic pressure dependent of the static dielectric function of Si, Ge, and GaAs**

Figure 7 and 8 presents the hydrostatic pressure dependence of the static dielectric function,  $\epsilon_\infty$ , of Si, Ge, and GaAs calculated within the LDA without and with the scissors-operator shift (SOS), respectively. Our data are compared to the experimental results of Goñi *et al.* [1] and to the pseudopotential calculations of Si and Ge of Levine and Allan [6]. Our calculation and the pseudopotential theory of Ref. [6] suggest that LDA is overestimating the static dielectric function of Si, Ge, and GaAs over the whole range of hydrostatic pressure, and that the use of a unique value of the scissors-operator shift for the correction of the band gap at  $\Gamma$  produces a nice agreement with the experimental results [1]. The static dielectric function decreases almost linearly with the pressure due to the increase of the direct band gap. However, for Si  $\epsilon_\infty$  is almost constant with the pressure and this is because the increase of the direct band gap is almost compensated by a decrease of the indirect band gap (see Figure 2).

Table V, VI, and VII present the calculated pressure band gaps, static dielectric function and f-sum rule for Si, Ge, and GaAs, with a comparison to the experimental results of Ref. [1]. The agreement with the experimental results is excellent when the scissors-operator shift is used. The f-sum rule deviates at most by 5.2% from unity in the case of Ge which reflect the high precision of the calculation of the optical matrix elements. The fact that the f-sum rule is not quite exhausted for Ge and GaAs (deviation of about 5%) as compared to Si (deviation of about 1%) is not due to a possible incompleteness of our basis set [36] but rather to our use of all electron electronic structure. When the valence states are very well isolated from the core states, like in the case of Si where the core states lie about

80 eV below the valence bands, the sum rule should be exhausted. However, for Ge and GaAs where the semi-core  $3d$ -states are very close to the valence states and greatly affect the optical properties, the f-sum rule could deviate markedly from unity, i.e., the average effective number of electrons per atom contributing to the optical transitions is much larger than 4 electrons per atom [37]. In pseudopotential theory, since the core states are absent, the f-sum rule is exhausted for all semiconductors [6]. The details of the contribution of the  $3d$  semi-core states to the oscillator strength and the study of the effective number of electrons contributing to the optical transitions are out of the scope of this paper and will be addressed elsewhere.

The first and second-order coefficients describing the pressure dependence of the static dielectric function  $\epsilon_\infty$  are presented in Table VIII. The results are compared to the experimental results of Goñi et al. Ref. [1], and the pseudopotential calculation of Ref. [6]. The overall agreement with experiment and the pseudopotential calculation is excellent.

In Table IX we present our calculation for the static dielectric function of Si, Ge, and GaAs including the spin-orbit coupling effect at the variational level, and the effect of the  $3d$  states in the interband transitions. The calculated potential includes always the  $3d$  states, and only the dielectric function is calculated with or without the  $3d$  interband transitions. We have obtained that the inclusion of the  $3d$  interband transitions increases slightly the static dielectric function, whereas the spin-orbit coupling increases it by 2.1% and 3.2% for Ge and GaAs, respectively. The  $\epsilon_\infty$  of Si is insensitive to the spin-orbit coupling. The calculated scissors-operator shift  $\epsilon_\infty$  including the spin-orbit coupling effect decreases by about 3.3% and 4.1% for Ge and GaAs, respectively. This is because the band gaps of Ge and GaAs are further reduced in presence of spin-orbit coupling which resulted in a larger scissors-operator shift for the determination of  $\epsilon_\infty^{QP}$ .



## V. CONCLUSION

The macroscopic dielectric function in the random-phase-approximation without local field effect has been implemented using the local density approximation with an all electron, full-potential linear muffin-tin orbital orbital basis-set. The method is used to calculate the optical properties of the semiconductors, Si, Ge, and GaAs, under hydrostatic pressure. We have found that the LDA overestimates the static dielectric function over all the pressure range from 0 to 12 GPa, and that a single value of the so called scissors-operator shift which account for the correct band gap at  $\Gamma$  produced a good agreement with the experimental data of Goñi and coworkers [1]. This makes us conclude that because LDA underestimates the band gap it is incapable of producing the correct static dielectric function even though  $\epsilon_\infty$  is a ground state property.

Since (i) the Kohn-Sham (KS) density functional (DF) without the local density approximation should in principle produce the correct  $\epsilon_\infty$ , and (ii) since the LDA calculation with the scissors-operator shift also produces the correct  $\epsilon_\infty$ , we are tempted to conclude that the KS-DF theory should produce the correct band gap for semiconductors. This conclusion is not confirmed by a non-selfconsistent GW calculations which suggest that the true KS-DF theory also underestimates the band gap [18].

Our analysis of the dielectric function, the sum rules and the energy-loss function shows that while the scissors-operator shift is a good approximation for the low lying excited states it appears as bad approximation for the high energy excited states. This is because the high energy states are free electron like hence well described within LDA.

Our calculation of the dynamical dielectric function shows that the  $E_1$  peak intensity is underestimated for Si by about 50%, and for Ge and GaAs by only 12%. These results imply that the excitonic effects may be important for the dielectric function of Si, but less for those for Ge, and GaAs.

We have also shown that including the  $3d$  semi-core states in the interband transitions hardly changes the static dielectric function,  $\epsilon_\infty$ , however their contribution to the intensity

of dynamical dielectric function for higher photon energies is substantial, and could be checked experimentally. We have also found that the spin-orbit coupling has a significant effect on  $\epsilon_\infty$  of Ge and GaAs, but not of Si.

We thank J. W. Wilkins for interesting discussions. This research was supported in part by the U.S. Department of Energy Basic Energy Sciences, Division of Materials Sciences and by NSF, grant number DMR-9520319. Supercomputer time was provided by the Ohio State Supercomputer Center.

## REFERENCES

- [1] A. R. Goñi, K. Syassen, and M. Cardona, Phys. Rev. B **41**, 10104 (1990).
- [2] L. Viña, S. Logothetidis, and M. Cardona, Phys. Rev. B **30**, 1979 (1984).
- [3] D. E. Aspnes and A. A. Studna, Phys. Rev. B **27**, 985 (1983).
- [4] S. Baroni and R. Resta, Phys. Rev. B **33**, 7017 (1986).
- [5] M. Alouani, L. Brey, and N. E. Christensen, Phys. Rev. B **38**, 1138 (1987).
- [6] Z. H. Levine and D. Allan, Phys. Rev. B **43**, 4187 (1991); Phys. Rev. Lett. **66**, 41 (1991).
- [7] A. Dal Corso, S. Baroni, and R. Resta, Phys. Rev. B **49**, 5323 (1994).
- [8] M. Chandrapal and F. H. Pollak, Solid State Comm. **18**, 1263 (1976), and Phys. Rev. B **15** 2127 (1977).
- [9] W. R. Hanke and L. J. Sham, Phys. Rev. Lett. **33**, 582 (1974); Phys. Rev. B **21**, 4656 (1980).
- [10] L. J. Sham, in *Proceeding of the Fifteenth International Conference on the Physics of semiconductors*, Kyoto, 1980 (J. Phys. Soc. Jpn. Suppl. A **49**, 69 (1980)).
- [11] W. Hanke, H. J. Mattausch, and G. Strinati, in *electron correlations in solids, molecules, and atoms*, edited by J. T. Devreese and F. Brosens (Plenum Publishing corporation, 1983).
- [12] M. del Castello-Mussot and L. J. Sham, Phys. Rev. B **31**, 2092 (1985).
- [13] S. G. Louie, J. R. Chelikowsky, and M. L. Cohen, Phys. Rev. Lett. **34**, 155 (1975).
- [14] P. Hehenberg et W. Kohn, Phys. Rev. **136**, B864 (1964); W. Kohn et L. J. Sham, Phys. Rev. **140**, 1133 (1965).
- [15] U. Von Barth and L. Hedin, J. Phys. C **5**, 1629 (1972).

- [16] L. Hedin, Phys. Rev. **139**, A796 (1965).
- [17] M. S. Hybertsen and S. G. Louie, Phys. Rev. B **34**, 5390 (1986).
- [18] R. W. Godby, M. Schlüter, and L. J. Sham, Phys. Rev. B **37**, 10159 (1988).
- [19] J. P. Perdew and M. Levy, Phys. Rev. Lett. **51**, 1884 (1983); R. W. Godby, M. Schlüter, and L. J. Sham, Phys. Rev. Lett. **56**, 2415 (1986).
- [20] C. S. Wang and B. M. Klein, Phys. Rev. B **24**, 3417 (1981).
- [21] M. Huang and W. Y. Ching, Phys. Rev. B **47**, 9449 (1993).
- [22] O. K. Andersen, Phys. Rev. B **12**, 3060 (1975).
- [23] J. M. Wills, unpublished.
- [24] Here the principal quantum number  $\nu$  and the spin channel  $\sigma$  are ignored for simplicity, however our numerical code has the spin polarization capability, and the use of the different  $\nu$  with the same momentum channel in the basis set. We use also only one  $\kappa$  variational parameter per orbital (see definition in the text) in all formulas to avoid using it as an obvious index to the wave function and extra summation in the Bloch wave function.
- [25] G. B. Bachelet and N. E. Christensen, Phys. Rev. B **31**, 879 (1985).
- [26] N. E. Christensen, Phys. Rev. B **30**, 5753 (1984).
- [27] C. T. Chan, D. Vanderbilt, and S. G. Louie, Phys. Rev. B **33**, 2455 (1986).
- [28] M. Rohlfing, P. Krüger, and J. Pollmann, Phys. Rev. B **48**, 17791 (1993).
- [29] S. L. Adler, Phys. Rev. **126**, 413 (1962); N. Wiser, Phys. Rev. **129**, 62 (1963).
- [30] H. Ehrenreich and M. L. Cohen, Phys. Rev. **115**, 786 (1959).
- [31] O. Jepsen et O. K. Andersen, Solid State Commun. **9**, 1763 (1971); G. Lehmann et M.

- Taut, Phys. Stat. Sol. **54**, 469 (1972).
- [32] A. B. Chen, Phys. Rev. B **14**, 2384 (1976).
- [33] R. Del Sole and R. Girlanda, Phys. Rev. B **48**, 11789 (1993).
- [34] M. Methfessel, Phys. Rev. B **38**, 1537 (1988).
- [35] J. R. Chelikowsky and M. L. Cohen, Phys. Rev. Lett. **31**, 1582 (1973).
- [36] We have checked carefully the basis set by increasing the number of Hankel functions for negative kinetic energies and Neumann functions for positive kinetic energies  $\kappa^2$  and have not been able to improve on the f-sum rule. Our basis-set indicates that all physical properties quantities have been converged, including the total energy which is converged at the tenth of the mRy level.
- [37] For more information see H. R. Philipp and H. Ehrenreich, Phys. Rev. **129**, 1550 (1963).
- [38] W. A. Harrison, *Electronic structure and the properties of solids*, (Freeman, San Francisco, 1980).
- [39] H. H. Li, J. Chem. Phys. Data **9**, 561 (1980).

## FIGURES

FIG. 1. Calculated energy-loss function of GaAs within the LDA (full curve) and within the scissors approximation (dashed curve). It is clearly seen that the maximum of the LDA curve is much closer to the free valence electron plasma frequency of 15.5 eV.

FIG. 2. Calculated (a) direct band gap  $E_0$ , and (b) minimum band gap  $E_{\text{gap}}$  of Si, Ge, and GaAs as a function of hydrostatic pressure compared to the experimental results of Goñi *et al.* [1] for Ge (dashed line), and GaAs (thick line). Plot (a) shows that the direct band gaps increase almost linearly with pressure. Plot (b) shows that for GaAs there is a cross over of the band gap from direct to indirect at around 8 GPa, and a cross over for Ge at almost 3 GPa. The indirect band gap of Si decreases linearly with pressure.

FIG. 3. Calculated imaginary part of the dielectric function of Si at the experimental equilibrium volume, shifted by  $\Delta = 0.6$  eV towards higher photon energies, compared with the experimental results of Ref. [3]. The experimental  $E_1$  structure at 4 eV is underestimated whereas the main  $E_2$  structure at 4.5 eV is overestimated.

FIG. 4. Imaginary part of the dielectric function of Ge at 10 kbar shift by 0.4 eV and GaAs at the experimental equilibrium volume shifted by 1.1 eV, compared with the experimental results of Ref. [3]. In both Ge and GaAs  $\epsilon_2(\omega)$  the experimental  $E_1$  is only slightly underestimated and  $E_2$  is overestimated.

FIG. 5. Contribution of the  $3d$  interband transitions to the imaginary part of the dynamical dielectric function of (a) Ge (at 10 kbar) and (b) GaAs at the experimental equilibrium volume. The full line and the dashed line are with and without  $3d$  interband transitions, respectively. Due to the narrow nature of the  $3d$  semi-core states of Ge, the intensity of  $\epsilon_2$  above 25 eV is very similar to the empty  $p$ -density of states of Ge. Whereas for GaAs, the  $3d$  semi-core states of Ga are relatively delocalized, which makes the intensity of  $\epsilon_2$  above 12 eV much different from the Ga empty  $p$ -density of states.

FIG. 6. Real part of the dielectric function of Ge (at 10 kbar) and GaAs, at the experimental equilibrium volume, compared with the experimental results of Ref. [3]. The analytic asymptotic limit, shown by the empty circles, matches nicely the calculated spectra above 10 eV.

FIG. 7. LDA scalar-relativistic calculated static dielectric function of Si, Ge, and GaAs as a function of hydrostatic pressure compared to the experimental results of Goñi *et al.* [1] and the pseudopotential calculation of Levine and Allan [6].

FIG. 8. LDA plus the scissors-operator shift (SOS) calculated static dielectric function of Si, Ge, and GaAs as a function of hydrostatic pressure compared to the experimental results of Goñi *et al.* [1].

## TABLES

TABLE I. Basis-sets used for the calculation of the excited states of Si, Ge and GaAs. Each orbital has different kinetic energy  $\kappa^2$  in its the interstitial region. For example, the 3s orbital of Si is used three times, each of the 3s wave function has a different kinetic energy in the interstitial region.

Si:	$3 \times (3s, 3p)$	$2 \times (3d)$
	$3 \times (4s, 4p)$	$2 \times (4d, 4f)$
Ge:		$2 \times (3d)$
	$3 \times (4s, 4p)$	$2 \times (4d)$
		$2 \times (5s, 5p)$
GaAs:		$2 \times (Ga\ 3d)$
	$3 \times (Ga\ 4s, 4p)$	$2 \times (Ga\ 4d)$
		$3 \times (Ga\ 5s, 5p)$
	$3 \times (As\ 4s, 4p)$	$2 \times (As\ 4d)$
		$3 \times (As\ 5s, 5p)$



TABLE II. Eigenvalues of Si at high symmetries points ( $\Gamma$ ,  $X$ , and  $L$ ) as compared to the results produced by means of a linear combination of gaussian orbitals [28], and by pseudopotential (PP) method [27]. The zero of energy is chosen at  $\Gamma_{25v'}$  point.

High-symmetry point	Gaussian orbitals	PP	Present Calculation
$\Gamma_{1v}$	-11.91	-11.91	-11.96
$\Gamma_{25v'}$	0.0	0.0	0
$\Gamma_{15c}$	2.57	2.55	2.56
$\Gamma_{2c'}$	3.24	3.28	3.20
$X_{1v}$	-7.77	-7.76	-7.82
$X_{4v}$	-2.78	-2.86	-2.83
$X_{1c}$	0.65	0.66	0.62
$X_{4c}$	10.03		10.03
$L_{2v'}$	-9.58	-9.56	-9.63
$L_{1v}$	-6.94	-6.96	-6.99
$L_{3v'}$	-1.17	-1.20	-1.19
$L_{1c}$	1.47	1.50	1.44
$L_{3c}$	3.32	3.33	3.31
$L_{2c'}$	7.77		7.66
Indirect band gap	0.52		0.50

TABLE III. Calculated equilibrium volume ( $V$ ), electronic pressure, and bulk modulus of Si, Ge, and GaAs. The the bulk modulus are calculated both at the experimental ( $V_0$ ) and theoretical ( $V$ ) unit cell volumes. The experimental results are shown between parenthesis.

Semiconductor	$V_0$ ( $\text{\AA}^3$ )	$V/V_0$	$P(V_0)$ (GPa)	$B(V)$ (GPa)	$B(V_0)$ (GPa)
Si	39.98	.990	-.70	95.8	91.2 (98.8)
Ge	45.27	.988	-.80	71.0	67.1 (74.4)
GaAs	45.12	.984	-1.2	74.2	69.3 (74.7)

TABLE IV. First and second-order coefficients describing the dependence of the direct band gap at  $\Gamma$  ( $E_0$ ) under hydrostatic pressure ( $E_0(P) = E_0 + aP + bP^2$ ) for Si, Ge, and GaAs. The experimental results are from Goñi et al. Ref. [1].

	$E_0$		a (meV/GPa)		b (meV/GPa <sup>2</sup> )	
	Theory	Expt.	Theory	Expt.	Theory	Expt.
Si	3.273		100.8		0.05	
Ge	-0.084	0.795	125.4	121	0.2	0.2
GaAs	0.41	1.43	99.1	108	-0.1	-0.1

TABLE V. Calculated pressure, band gap, static dielectric function with and without scissors-operator shift (SOS), and the f-sum rule of Si as a function of volume. [28],

$V_0/V$	P(GPa)	f-sum	gap(eV)	$\epsilon_\infty$ (LDA)	$\epsilon_\infty$ (SOS)	$\epsilon_\infty$ (Expt.)
1.000	-.75	0.988	0.50	13.75	12.08	12.0 <sup>a</sup>
1.025	1.8	0.989	0.46	13.65	12.00	
1.050	4.8	0.987	0.42	13.61	11.96	
1.100	9.8	0.991	0.34	12.57	11.98	

<sup>a</sup> Ref. [38]

TABLE VI. Calculated pressure, band gap, static dielectric function with and without scissors-operator shift (SOS), and the f-sum rule of Ge as a function of volume. The experimental data are from Goñi et al. [1].

$V_0/V$	P(GPa)	f-sum	gap(eV)	$\epsilon_\infty$ (LDA)	$\epsilon_\infty$ (SOS)	$\epsilon_\infty$ (Expt.)
1.025	1.0	1.053	.04	19.24	15.32	15.59
1.050	2.9	1.041	.21	18.14	14.71	15.01
1.075	5.0	1.042	.29	17.44	14.33	14.49
1.100	7.2	1.043	.37	16.70	13.90	14.07
1.150	12.3	1.045	.48	15.81	13.46	13.63

TABLE VII. Calculated pressure, band gap, static dielectric function with and without scissors-operator shift (SOS), and the f-sum rule of GaAs as a function of volume. The experimental data are from Goñi et al. [1].

$V_0/V$	P (GPa)	f-sum	gap(eV)	$\epsilon_\infty$ (LDA)	$\epsilon_\infty$ (SOS)	$\epsilon_\infty$ (Expt.)
1.000	-1.2	1.041	.29	14.44	11.0	11.05
1.025	.68	1.042	.48	13.93	10.72	10.88
1.050	2.8	1.043	.66	13.45	10.53	10.69
1.075	4.7	1.044	.85	13.09	10.41	10.53
1.100	6.8	1.044	1.02	12.75	10.25	10.34
1.150	11.8	1.046	1.08	12.20	10.03	9.90

TABLE VIII. First and second-order coefficients describing the dependence of the static dielectric function on hydrostatic pressure ( $\epsilon_\infty(P) = \epsilon_\infty^0 + aP + bP^2$ ) for Si, Ge, and GaAs. The experimental data are from Goñi et al. [1].

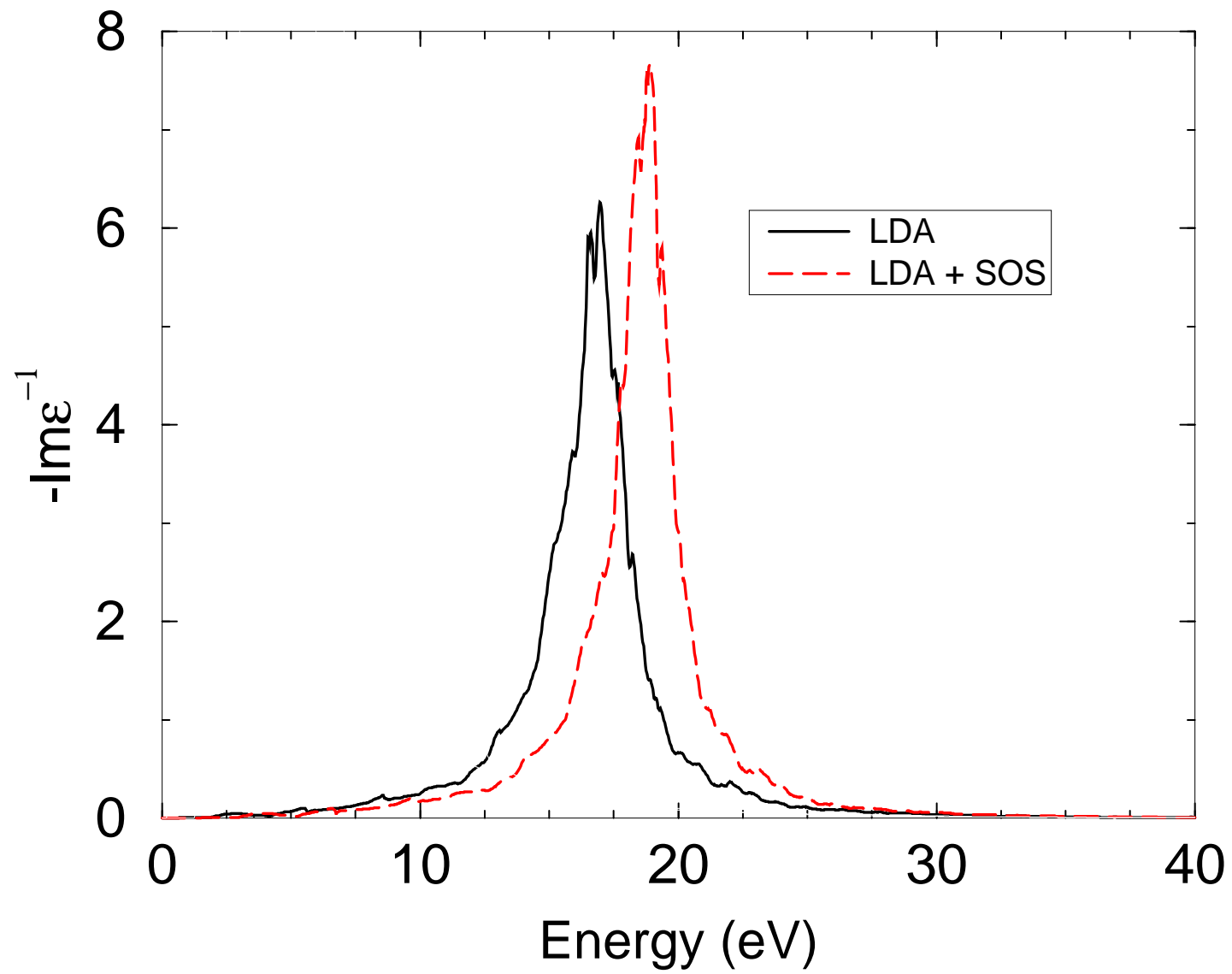
	$\epsilon_\infty^0$		a(1/GPa)		b (1/GPa <sup>2</sup> )		$d \ln(\epsilon_\infty)/dP(10^{-12}/\text{Pa})$	
	Theory	Expt.	Theory	Expt.	Theory	Expt.	Theory	Expt.
Si	12.05		-0.032		0.0025		-2.65	
Si	11.16 <sup>a</sup>		-0.027 <sup>a</sup>		0.0013 <sup>a</sup>		-2.6,-2.43 <sup>a</sup>	
Ge	15.58	15.94	-0.32	-0.36	0.012	0.014	-20.21	-22.60
	16.04 <sup>a</sup>		-0.46 <sup>a</sup>		0.018 <sup>a</sup>		-31,28.66 <sup>a</sup>	
GaAs	10.83	10.92	-0.11	-0.09	0.004		-10.43	-8.06

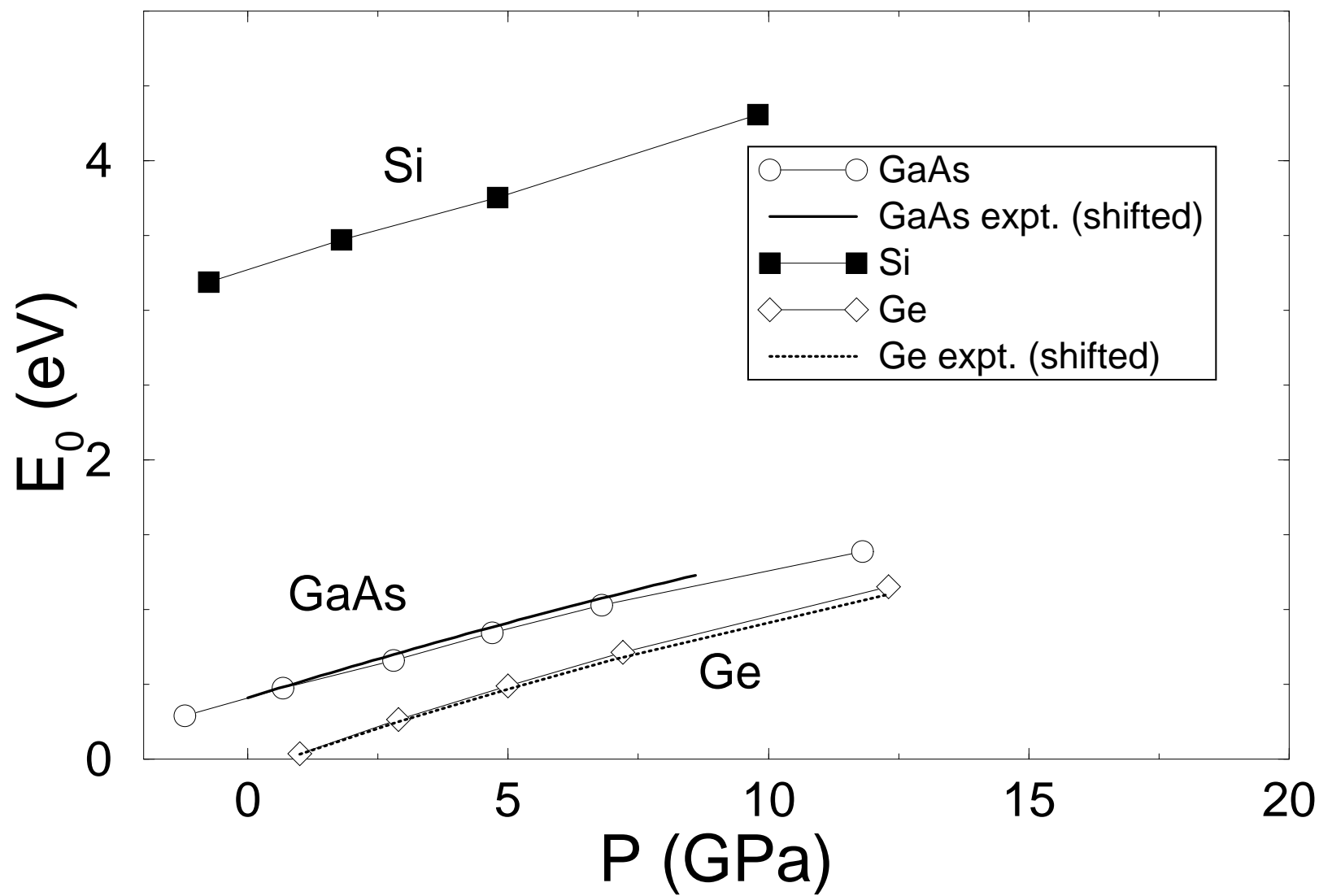
<sup>a</sup> Pseudopotential calculation of Ref. [6], slightly larger numbers are quoted for  $d \ln(\epsilon_\infty)/dP$  in their Table VI.

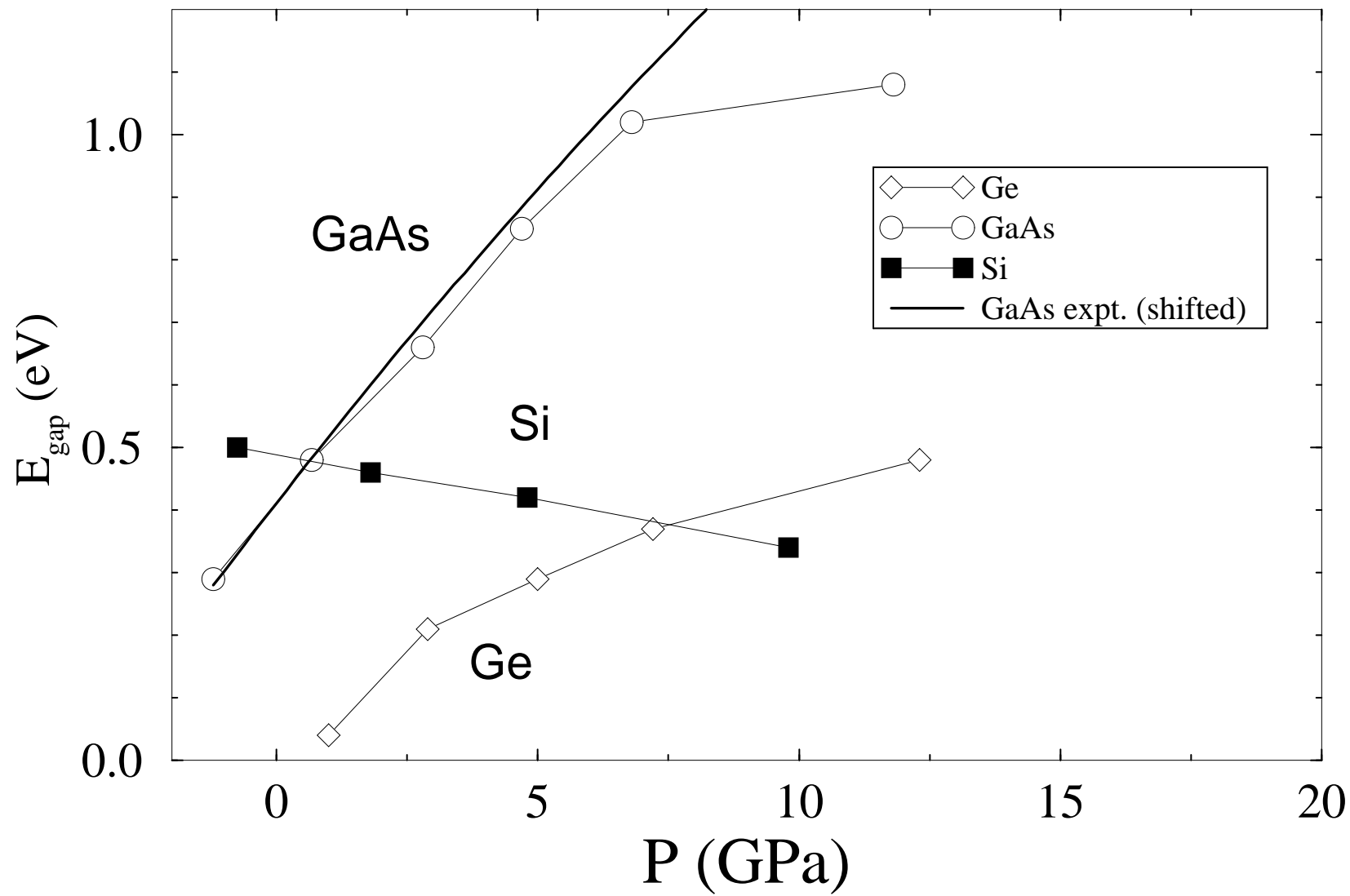
TABLE IX. Calculated static dielectric function of Si, Ge, and GaAs at the equilibrium lattice parameter (except for Ge where it is calculated at a slightly smaller lattice parameter (1% smaller) than the experimental one because Ge is a metal in LDA for  $V/V_0 = 1$ ). The calculation are done using scalar relativistic (SR) LMTO without  $3d$  states, with the  $3d$  states (SR+ $3d$ ), with the spin-orbit coupling at the variational level (SR+SO), and with the SO coupling and the  $3d$  states included (SR+SO+ $3d$ ).

	Si		Ge		GaAs	
	LDA	LDA+SOS.	LDA	LDA+SOS	LDA	LDA+SOS
SR	13.75	12.08	18.14	14.71	14.44	11.0
SR+ $3d$			18.16	14.73	14.47	11.03
SR+SO	13.69	12.0	18.52	14.23	14.90	10.52
SR+SO+ $3d$			18.54	14.25	14.93	10.55
Expt.		12.0 <sup>a</sup> 11.4 <sup>b</sup>		14.98 <sup>c</sup>		10.9 <sup>a</sup>

<sup>a</sup> Ref. [38]    <sup>b</sup> Ref. [39]    <sup>c</sup> Ref. [1]

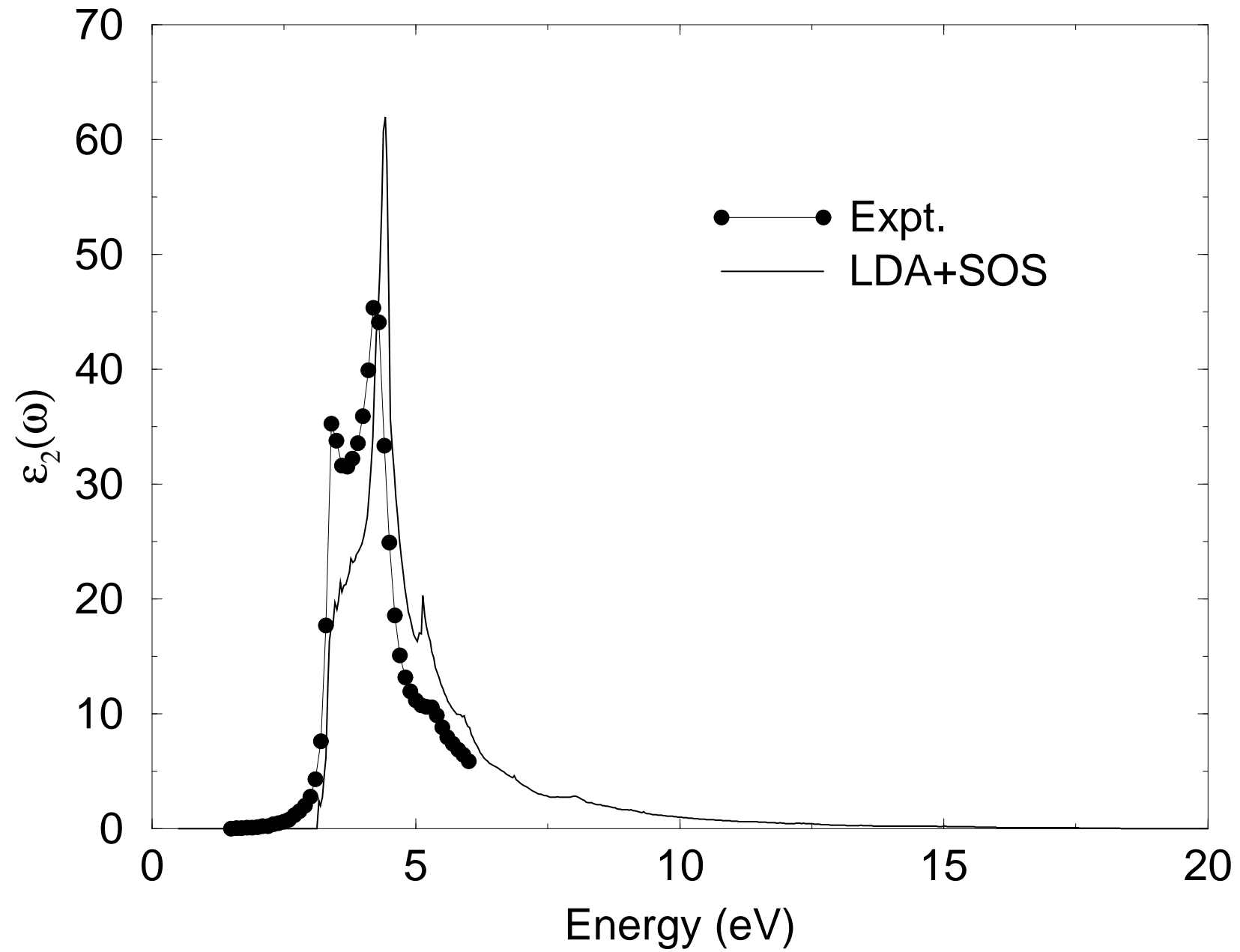




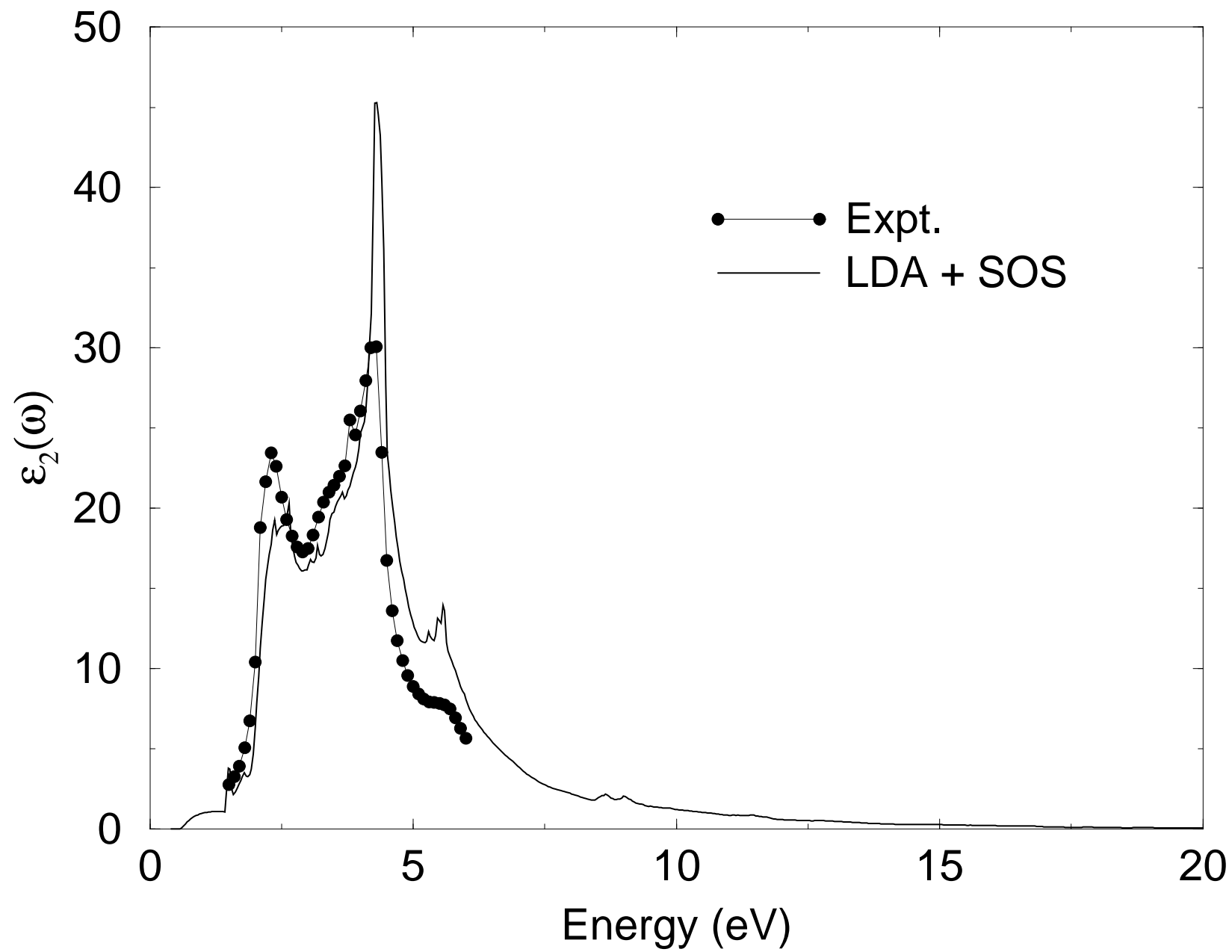




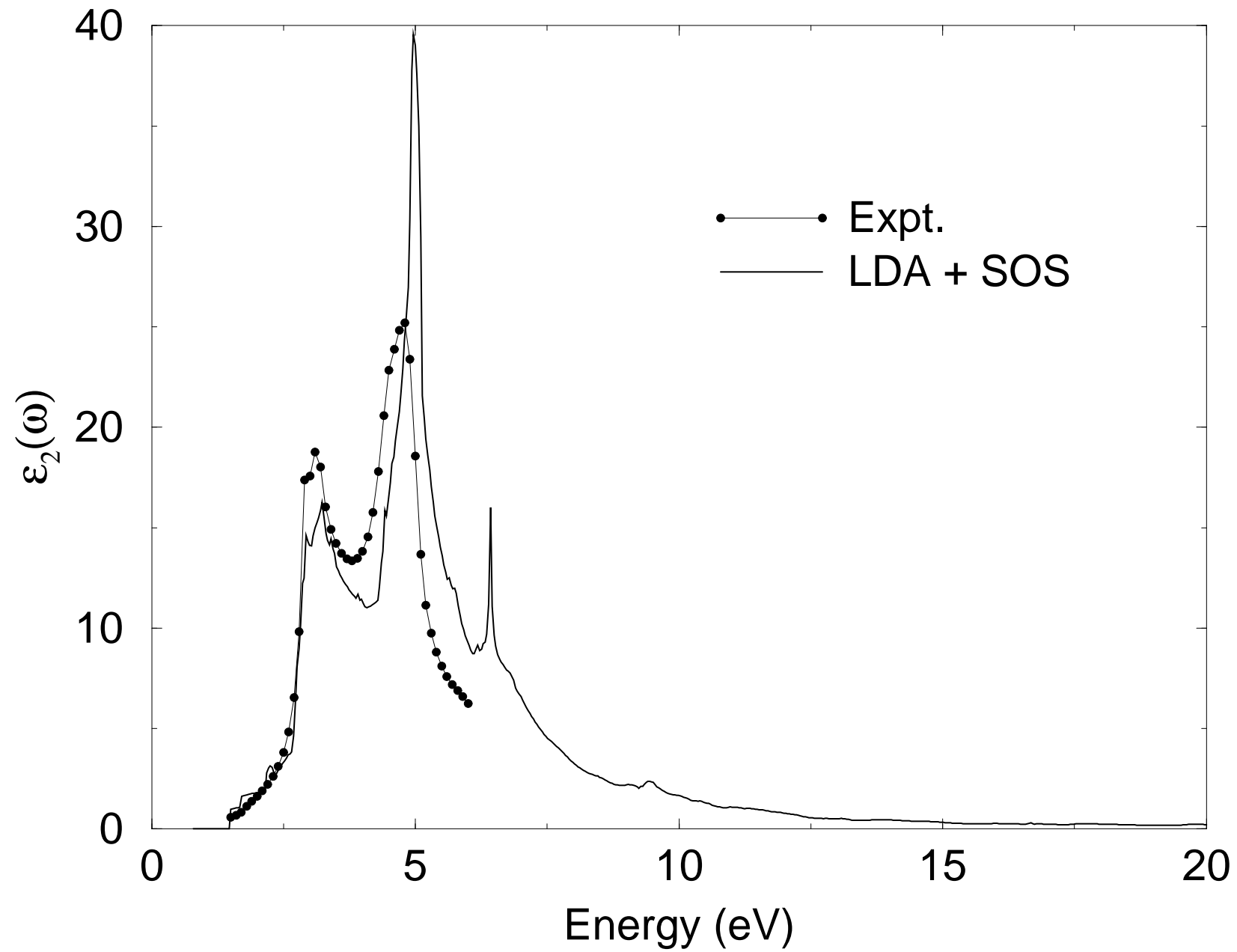
# $\epsilon_2$ of Si

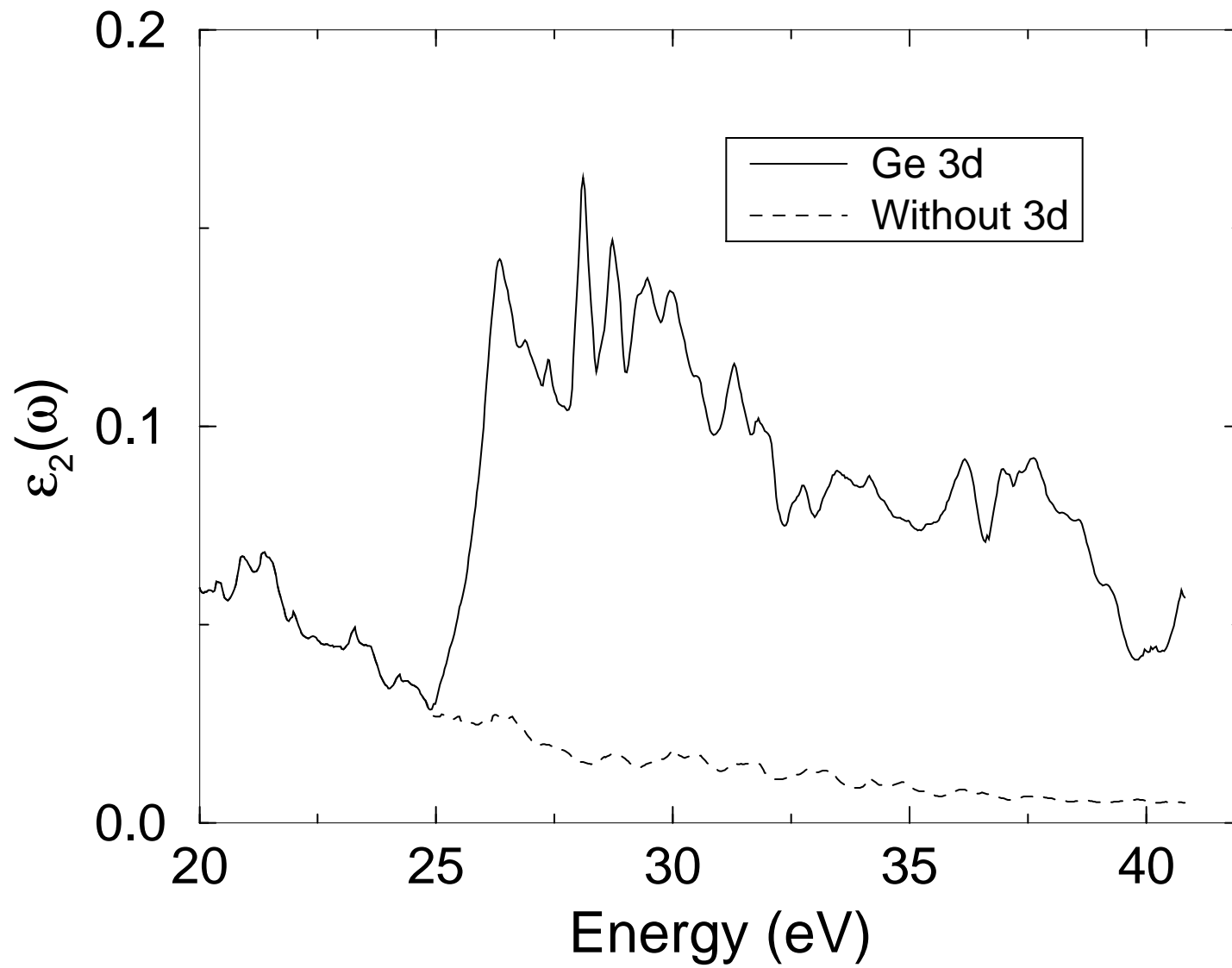


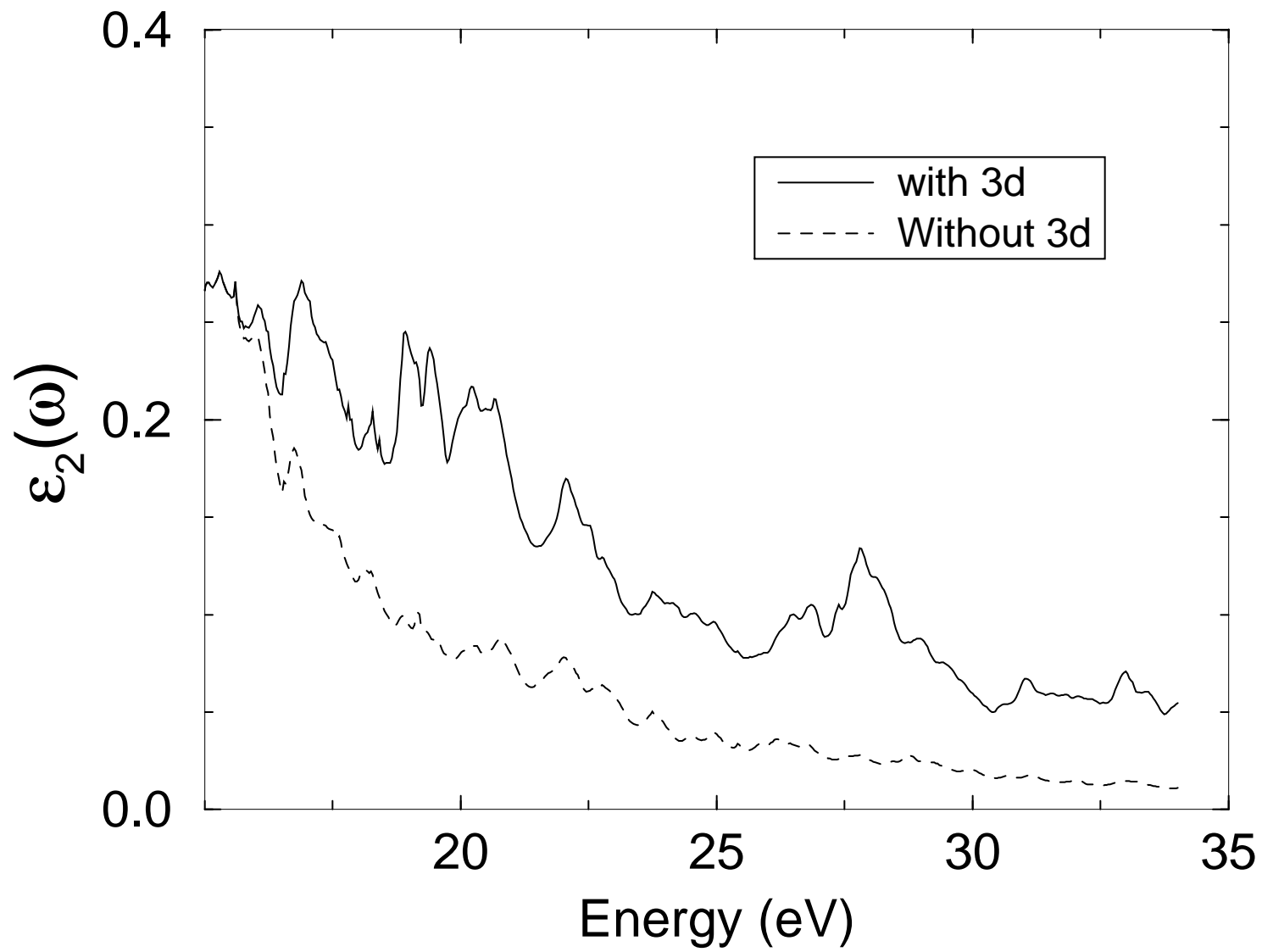
# $\epsilon_2$ of Ge



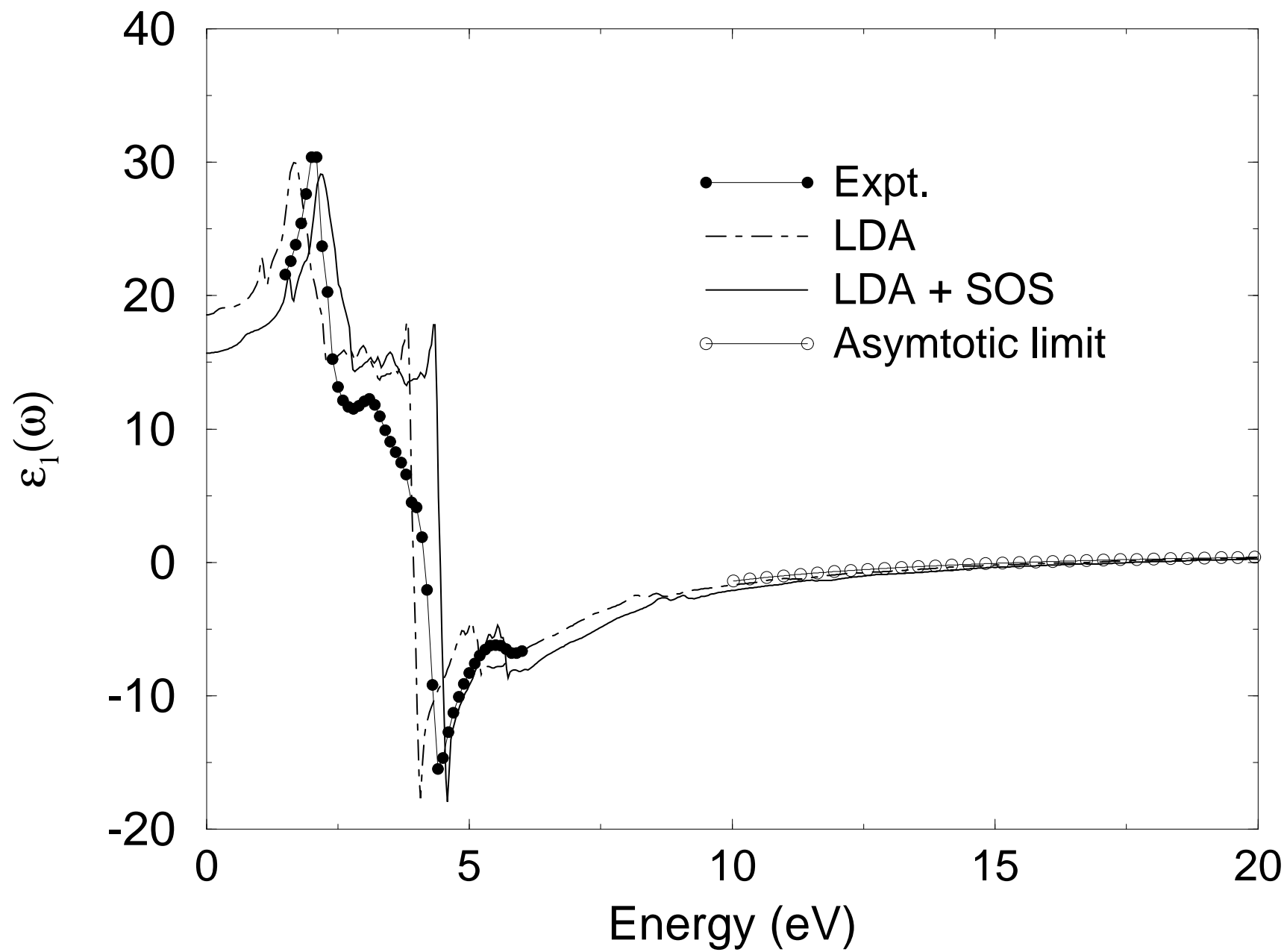
# $\epsilon_2$ of GaAs







# $\epsilon_1$ of Ge



# $\epsilon_1$ of GaAs

